

XRD and W-H analysis of sol-gel synthesized iron doped Zn-Cr oxide nanoparticles.

¹S. D. Balsure, ²Mahesh Gurav, ³S. T. Alone, ⁴Vikram More, ⁵A. B. Kadam

¹Research Scholar, ²Research Scholar, ³Head and Assistant Professor, ⁴Research Scholar, ⁵Research Guide and Associate Professor

^{1,5}Department of Physics, Jawahar Mahavidyalaya, Anadur, Osmanabad (M.S.) India

²Department of Chemistry, SMP College, Murum, Osmanabad (M.S.) India

^{3,4}Department of Physics, R. S. College, Pathri, Aurangabad (M.S.) India

Email: ⁵drabkadam@gmail.com

Abstract: Zinc oxide nanoparticles have unique optical properties which have promising applications in luminescent devices. Pure and doped zinc oxides have several applications due to their unique structural and optical properties. Iron substituted Zn-Cr nano oxides were prepared by using the sol-gel auto-combustion method. X-ray diffraction patterns confirm the wurtzite crystal structure of the samples belonging to hexagonal crystal symmetry. Lattice constant 'a' varies from 3.2487Å to 3.2474Å and 'c' varies from 5.2043Å to 5.2029Å. Crystallite size was calculated by using well known Scherrer equation and W-H plots and it was observed within the nanometer range. The Williamson-Hall method was used to understand the changes observed in lattice strain. For $x \leq 0.02$, negative strain values are observed indicating the compressive type and for $x > 0.02$, positive strain values indicating the tensile type of strain.

Key Words: Zinc oxide, lattice constant, crystallite size, W-H analysis.

INTRODUCTION:

Oxide semiconductors play an important role in the field of research because of their versatile applications in recent technology. These materials exhibit particle size dependent properties and therefore can be considered as the key materials in the technologically important components [1]. Recently, the demand of nano-sized semiconductors is increased because of their unique optical and electrical properties which are mostly useful in the fabrication of nano-sized multifunctional optoelectronic and electronic devices [2-5]. Among the metal oxides, zinc oxide has a commercial importance due to its major use in paints, rubber, catalyst, sensors, varistors as it exhibits semiconducting, piezoelectric and pyroelectric properties [6, 7]. Zinc oxide in nano-size has potential applications due to its altered properties than that of bulk size. Doping of various metal ions dramatically changes the structural, optical and electrical properties of zinc oxides [8-10].

In the recent past, several chemical methods have been employed to obtain the zinc oxide nanostructures by many researchers which includes chemical vapor deposition [11], thermal evaporation [12], hydrothermal [13], sol-gel auto ignition [14], electrochemical deposition [15], laser ablation [16], and sputter deposition [17]. In the present study we have adopted the sol-gel auto-ignition route in order to obtain the iron doped Zn-Cr oxide nanoparticles. The structural properties were studied by using X-ray diffraction method. Crystallite size and micro-strain observed in the samples were studied by using W-H analysis.

EXPERIMENTAL:

Nanoparticles of iron doped Zn-Cr oxide nanoparticles having general chemical formula $Fe_xZn_{0.9-x}Cr_{0.5}O$ ($x = 0.0, 0.02, 0.04, 0.06, 0.08$ and 1.0) were obtained by using sol-gel auto-ignition method. Analytical graded metal nitrates with high purity (Zinc nitrate, iron nitrate, and chromium nitrate) of the constituent elements were used as starting materials. All the starting materials were mixed with their weight proportion in sufficient amount of double distilled water. Citric acid was used as chelating agent and liquid ammonia was poured slowly in the solution to maintain the pH=7. Whole mixture was kept on hot plate and continuously stirrer at constant temperature of 90°C. After couple of hours the solution becomes denser and the viscosity of the solution suddenly decreases and it converts into viscous sol. After few minutes the viscous sol converted into dried gel and burnt into ash by auto-ignition process. The burnt ash then sintered at 850°C in order to obtain the final product in the form of fine particles at nano-scale level. The newly prepared samples were characterized by using X-ray diffraction technique. Room temperature XRD patterns of all the samples were collected in the 2θ range of 20° to 80° by using Cu-K α radiations of wavelength 1.5405 Å.



Principal Page 110

RESULTS AND DISCUSSION:

Fig. 1 represents the X-ray diffractograms of $Fe_xZn_{0.95-x}Cr_{0.05}O$ nanoparticles. Diffraction peaks indexed for the planes (100), (002), (101), (102), (110), (103), (200), (112), (201), (004), and (202) are attributed to zinc oxide corresponds to the hexagonal (wurtzite) crystal structure of the samples. The secondary phase of Cr_2O_3 and Fe_2O_3 were also observed in the X-ray diffraction patterns of the samples. Broadening of the Bragg's lines clearly indicates the nanocrystalline nature of the samples. Lattice parameters 'a' and 'c' of all the samples were evaluated by using the following relation [18],

$$\frac{1}{d^2} = \frac{4}{3} \left(\frac{h^2 + hk + k^2}{a^2} \right) + \frac{l^2}{c^2} \tag{1}$$

When, $h = 0$ and $k = 0$ (i.e. for the planes (002) and (004)) then lattice parameter 'c' can be evaluated by using following relation,

$$c = ld \tag{2}$$

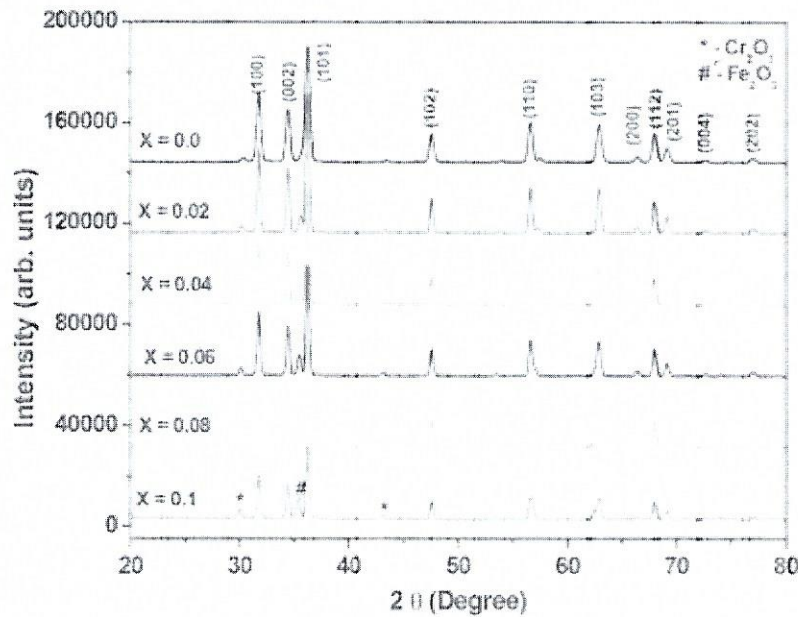


Fig. 1: X-ray diffraction patterns of $Fe_xZn_{0.95-x}Cr_{0.05}O$ nanoparticles

Calculated values of lattice parameters 'a' and 'c' for all the samples of the series $Fe_xZn_{0.95-x}Cr_{0.05}O$ are listed in Table 1. It can be seen that the lattice parameter 'a' decreases from 3.2487 Å to 3.2474 Å and 'c' decreases from 5.2043 Å to 5.2029 Å. The decrease in lattice parameter by the addition of Fe ions can be explained on the basis of difference in ionic radii. Here in the present series Fe ions having ionic radii 0.67 Å replaces the Zn ions having relatively larger ionic radii 0.83 Å [19]. The replacement of larger ions by smaller one reduces the size of unit cell and hence cell parameters decreases.

Table 1: Lattice constant (a), X-ray density (d_x), crystallite size (t) (XRD and W-H analysis), and micro-strain observed in $Fe_xZn_{0.95-x}Cr_{0.05}O$.

'x'	Lattice Parameter		'V' (Å) ³	'd _x ' (gm/cc)	't' (nm)		Strain
	'a' (Å)	'c' (Å)			XRD	W-H analysis	
0.0	3.2487	5.2043	47.599	5.6352	17.565	17.81	-1.569×10^{-4}
0.02	3.2485	5.2041	47.590	5.6229	22.878	23.90	-3.848×10^{-6}
0.04	3.2482	5.2039	47.581	5.6106	23.014	25.45	2.089×10^{-4}
0.06	3.2479	5.2036	47.570	5.5985	23.204	26.92	3.133×10^{-4}
0.08	3.2476	5.2032	47.558	5.5866	23.277	27.90	5.150×10^{-4}
0.1	3.2474	5.2029	47.547	5.5745	23.443	28.85	5.950×10^{-4}

Unit cell volume of all the samples was estimated by using the relation $V = 0.866a^3c$ and the values are listed in Table 1. It can be observed that unit cell volume decreases with the substitution of Zn ions by Fe ions. This decrease in unit cell volume is attributed to the decrease in cell parameters. X-ray density was computed by using the relation discussed elsewhere [20] and it was obtained in the decreasing trend. The average crystallite size (t) was estimated by using the FWHM (β) values and Bragg's angles (θ_B) in well known Scherrer equation [20]:

$$t = \frac{k\lambda}{\beta \cos \theta_B} \quad (3)$$

where, λ is the wavelength of incident radiation (1.5405Å) and k is constant. Computed values of average crystallite size ' t ' varies from 17.565 nm to 23.443nm showing increasing trend with the addition of Fe ions in Zn-Cr oxides. The result indicates that the variation average crystallite size strongly depends on the Fe concentration. Increasing concentration of Fe ions promotes the crystallite growth. To confirm the nanocrystalline nature of the samples, Williamson-Hall method, which is another approach to estimate the average crystallite size was, employed [21]. This method gives the better information of crystallite size and contributions of micro-strains observed in the crystal lattice. By using the following W-H relation average crystallite size and micro-strain was obtained [22]:

$$\beta \cos \theta = \left(\frac{K\lambda}{t_{W-H}} \right) + 4\epsilon \sin \theta \quad (4)$$

where, ϵ - is the micro-strain brought in the crystal lattice, λ -is the incident wavelength (1.5405Å), K is the shape factor ($K = 0.94$ for the crystal having uniform size) and t_{W-H} is the average crystallite size obtained by the W-H analysis. W-H graphs plotted between $\beta \cos \theta$ and $4\epsilon \sin \theta$ are shown in Fig. 2.

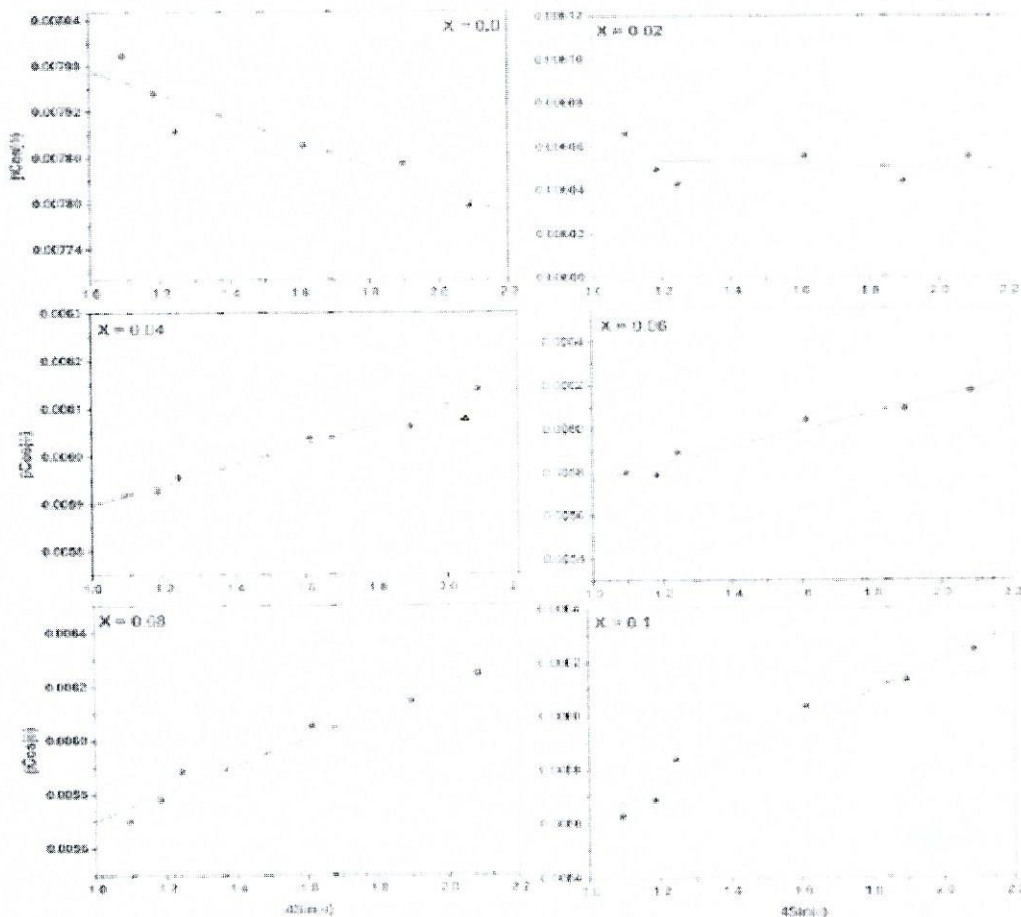


Fig. 2: W-H plots for the series $Fe_xZn_{0.95-x}Cr_{0.05}O$.

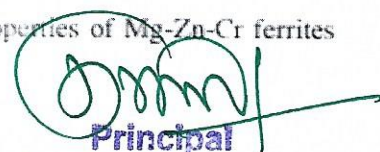
Average crystallite size from W-H plots was obtained from the Y-intercept and lattice strain was obtained from slope of the graph. The average crystallite size obtained from W-H plots increases from 17.81 nm to 28.85 nm which is in good agreement with the values obtained by using Scherrer equation. For the samples $x \leq 0.02$, the lattice strain shows negative values indicating the compressive type of strain in the crystal lattice. As the concentration of Fe ion increases from $x > 0.02$, positive values of micro-strain are observed which indicates the tensile type of strain in the crystal lattice.

CONCLUSIONS:

Oxide nanoparticles of $\text{Fe}_x\text{Zn}_{0.95-x}\text{Cr}_0.05\text{O}$ were successfully obtained by using sol-gel auto-ignition method. X-ray diffraction patterns confirm the hexagonal structure of the samples. Lattice parameter increases with the addition of Fe ions in Zn-Cr oxides which is related to the difference in ionic radii. Average crystallite size obtained from both Scherrer and W-H analysis is in nanometer range. For the samples $x \leq 0.02$, compressive type strain is observed and for $x > 0.02$, tensile type strain is observed in the crystal lattice.

REFERENCES:

- [1] V. D. Mote, Y. Puroshottam, B. N. Dole (2012); Williamson-Hall analysis in estimating of lattice strain in nanometer – sized ZnO particles; J. Theor. Appl. Phys. 06, 01-06
- [2] S. Talam, S. R. Karumari, N. Gunnam; Synthesis, characterization and spectroscopic properties of ZnO nanoparticles (2012); ISRN Nanotech. 2012; 1-6
- [3] M. S. Tokumoto, V. Briois, C. V. Santilli, S. H. Pulcinelli (2003); Preparation of ZnO nanoparticles: structural study of the molecular precursor; 26; 547-551.
- [4] P. Kumar, L. S. Panchakarla, S. V. Bhat, U. Maitra, K. S. Subrahmanyam, C. N. R. Rao (2010); Photoluminescence, white light emitting properties and related aspects of ZnO nanoparticles admixed with graphene and GaN; Nanotechnology 21; 385701.
- [5] G. Thomas, Invisible circuits (1997); Nature 389; 907-908.
- [6] Z. L. Wang; Nanostructures of zinc oxide (2004); Materials today 7; 26-33.
- [7] N. Tamaekong, C. Liewhiran, A. Wisitsoraat, S. Phanichphant; Flame-spray-made undoped zinc oxide films for gas sensing applications (2010); Sensors 10; 7865-7873.
- [8] Y. H. Heo, D. P. Norton, L. C. Tien; Low temperature patterned growth of ZnO nanorod arrays on Si (2004); Mater. Sci. Engg. R. Rep. 47; 1-47.
- [9] M. J. Height, L. Madler, S. E. Pratsinis, F. Krumeich; Nanorods of ZnO made by flame spray pyrolysis (2006); Chem. Mater. 18; 572-578.
- [10] E. Sommez, S. Aydin, M. Yilmaz, M. T. Yurtean, T. Karacali, M. Ertugrul, Study of structural and optical properties of zinc oxide rods grown on glasses by chemical spray pyrolysis (2011); J. Nanomater. 2012; 1-5.
- [11] K. Keis, E. Magnusson, H. Lindstrom, S. E. Lindquist, A. Hagfeldt; A 5% efficient photochemical solar cell based on nanostructured ZnO electrodes (2002); Solar Ener. Mater. Solar cells, 73; 51-58.
- [12] M. H. Hung, Y. Wu, H. Feick, N. Tran, E. Weber, P. Yang; Catalytic growth of zinc oxide nanowires by vapor transport (2001); Adv. Mater. 13; 113-116.
- [13] W. Lee, M. C. Jeong, J. M. Myoung; Catalyst free growth of ZnO nanowires by metal organic chemical vapor deposition and thermal evaporation (2004); Acta Mater. 52; 3949-3957.
- [14] S. E. Ahn, J. S. Lee, H. Kim; Photoresponse of sol-gel synthesized ZnO nanorods (2004); App. Phys. Lett. 84; 5022-5024.
- [15] Y. C. Wang, M. H. Hon; Preparation of nanosized ZnO arrays by electrophoretic deposition (2002); Elect. Solid State Lett. 5; 53-55.
- [16] Y. Sun, G. M. Fuge, M. N. R. Ashfold; ZnO/Zn phosphor thin films prepared by IBED (2004); Chem. Phys. Lett. 396; 21-26.
- [17] W. Chiou, W. Wu, J. Ting; Growth of single crystal ZnO nanowires using sputter deposition (2003); Dimo. Relat. Mater. 12; 1841-1844.
- [18] D. A. Vinnik, D. A. Zherebtsov, L. S. Mashkovtseva, S. Nemrava, N. S. Perov, A. S. Semisalova, I. V. Krivtsov, L. I. Isaenko, G. G. Mikhailov, R. Niewa (2014); Cryst. Grow. Des. 14; 5834.
- [19] S. E. Shirsath, S. M. Patange, R. H. Kadam, M. L. Mane, K. M. Jadhav; Structure refinement, cation site location, spectral and elastic properties of Zn^{2+} substituted NiFe_2O_4 (2012); J. Mol. Str. 1024; 77-83.
- [20] S. J. Haralkar, R. H. Kadam, S. S. More, S. E. Shirsath, M. L. Mane, S. D. Patil, D. R. Mane; Substitutional effect of Cr^{3+} ions on the properties of Mg-Zn ferrite nanoparticles (2012); Physica B 407; 4338-4346.
- [21] S. Debnath, K. Deb, B. Saha, R. Das, X-ray diffraction analysis for the determination of elastic properties of zinc-doped manganese spinel ferrite nanocrystals ($\text{Mn}_{0.95}\text{Zn}_{0.05}\text{Fe}_2\text{O}_4$), along with the determination of ionic radii, bond lengths, and hopping lengths (2019); J. Phys. Chem. Solids 134; 105-114.
- [22] M. Kuru, T. S. Kuru, E. Karaca, S. Bager; Dielectric, magnetic and humidity properties of Mg-Zn-Cr ferrites (2020); J. Alloys. Comp. 836; 155318.


Principal

Jawahar Arts, Science & Commerce College
Anapur, Tal. Tuljapur, Dist. Osmanabad.